ANIMAL WELL-BEING AND BEHAVIOR

The application of micro-CT in egg-laying hen bone analysis: introducing an automated bone separation algorithm

C. Chen and W. K. Kim[1]

Department of Poultry Science, University of Georgia, Athens, GA 30602

ABSTRACT The application of micro-CT in small animal research, especially on bone health, has risen exponentially in recent years. However, its application in egg-laying hen bone analysis was still limited. This review introduces the technical aspects of micro-CT in egg-laying hen bone analysis, especially with the medullary bones presented in the cavity. In order to acquate application of micro-CT for laying hen bone research, image acquisition, reconstruction, and analysis settings need to be adjusted properly. The key difference regarding the application of micro-CT in laying hen bone compared to other small animals such as mice and rats was the larger bone size and more complex structures of medullary and trabecular bones. In order to analyze the details of laying hen bone structures, the volume of interest for laying hen should be selected at a region where all 3 bones are present (critical, trabecular, and medullary bone). Owing to the complexity of bone structures, the conventional techniques are not useful to distinguish the trabecular bone and medullary bone in laying hens accurately. In the current review, an automated segmentation algorithm is described to allow researchers to segment bone compartments without human bias. The algorithm is designed according to the morphology difference of medullary bones compared to trabecular and cortical bones. In this procedure, the loosely woven bones were separated by applying dual thresholds. The medullary calcium chunks were separated by opening or closing procedures, where we defined the diameter of medullary chunks being higher than the trabecular bone thickness as a separation trait. The application of micro-CT in laying hen bone health assessment will significantly expand our understanding of chicken bone physiology and osteoporosis, contributing to improve welfare in laying hens.

Key words: micro-CT, laying hen bone, bone separation, 3D analysis

INTRODUCTION

Micro-CT is the "golden standard" for bone health assessment (Feldkamp et al., 1989). The application of micro-CT in research dramatically increased in recent years (Schambach et al., 2010). Compared to the clinic CT (voxel: ~ 1 mm^3), the micro-CT has a much higher resolution (as low as voxel: 1 μm^3) and higher sensitivity to detect subtle changes in the objects (Ritman, 2007). Previous literature showed many examples of the application of micro-CT on bone analysis of humans, mice, rats, and other species (Bouxsein et al., 2010; Schambach et al., 2010). However, micro-CT has not been widely used in poultry bone studies.

The conventional techniques used in poultry bone research were well-reviewed by Kim et al. (2012). Current evaluation methods for chicken bones include bone ash analysis, breaking strength test, dual-energy x-ray absorptiometry, and so on. The summary of advantages and limitations of these methods is present in Table 1. These traditional methods mainly focus on planar morphology evaluation and bone mass but ignored the structure of bones such as trabecular bone microarchitecture, which is highly correlated with bone strength (Siffert et al., 1996; Webber et al., 1998). An avian bone study demonstrated that more than 10% loss of trabecular bone could significantly impact the bone strain (Reich and Gefen, 2006), which suggests the integrity of trabecular bone to be critical for fracture resistance. The micro-CT is one of the methods which can capture detailed anatomical images of laying hen bones and build informative 3D models for structural analysis. This method will help the researcher better understand the distribution of mineral in bones and how 3D bone structure impacts bone fracture resistance.

Table 1. Summary of the advantages and limitations of bone quality analysis methods.

Methods	Advantage	Limitations
Bone ash analysis	- Low price - Easy to perform - Provide the information of bone mineral content	- Time consuming - Results can not reflect structural change of bones: pores, volume of bone cavity, and so on.
Bone breaking strength	- Provide the information of mechanical property of bones	- Results are affected by bone size, temperature, moister of samples
Histology	- Examine the details of internal architecture of various cells and tissues	- Time-consuming - Planar analysis - Subject to human error during the preparation and analysis of slides
Dual-energy X-ray absorptiometry (DEXA)	- Low radiation exposure - Allows for longitudinal studies - Provide additional parameters including soft-tissue composition	- Only measure areal bone mineral density - Resolution is lower than clinical CT and peripheral quantitative CT (pQCT) and micro-CT - Cannot distinct different parts of bones - The position of birds during scanning significantly affects the results
pQCT	- Volumetric bone mineral density - Bone separation at the cross-sections	- Cannot analysis bone 3D structures
Clinical computed tomography (clinical CT)	- Volumetric bone mineral density - 3D structural analysis - Can analysis large sample size/whole animal noninvasively	- Need large space to position the machine - lower resolution than micro CT
Micro computed tomography (micro-CT)	- Volumetric bone mineral density - 3D structural analysis - High definition - Segment analysis for each part of bones	- Has limitation on sample size - Time-consuming for high-definition scanning

Bouxsein et al. (2010) summarized the conventional methods and cautions, applications, and limitations of micro-CT for assessment of bone microarchitecture in rodents. However, while applying micro-CT to chicken bone structural analysis, some factors need to be adjusted carefully because of the unique chicken bone traits. In this review, the technical aspects of using micro-CT in laying hen bone analysis are introduced; the recommended settings for scanning, reconstruction, and analysis are interpreted; and a customized automated bone separation algorithm is introduced to meet the challenge of large quantities of data analysis in poultry research. This algorithm allows researchers to efficiently separate laying hen bones into the cortical, trabecular, and medullary regions with few user inputs. The segmented analysis can be applied to each part to obtain more defined data. The application of this method will expand our understanding of layer bone physiology in the future research.

THE ADVANTAGES AND LIMITATIONS OF MICRO-CT IN POULTRY BONE RESEARCH

The conventional optical or electron microscopy allows researchers to visualize 2-dimensional images of a bone biopsy surface or thin slices to obtain the inside structures, assuming that the structures are all plate-like. However, in most cases, a conclusion about 3-dimensional object structures cannot be made on the base of 2-dimensional information. The micro-CT system enables us to visualize and measure the true 3-dimensional object structures. These measurements include microarchitecture, true density, bone/tissue volume, 3-dimensional structural arrangement, and so on. Compared to conventional approaches, all quantitative parameters were calculated from 3-dimensional data without any model assumption. Korver et al. (2004) indicated that low to moderate correlations were observed in calculating bone mineral density (**BMD**) by using quantitative CT analysis (3D calculation) and traditional methods, such as bone ash. Moreover, the acquired images can be reconstructed to the 3D model and analyzed nondestructively (Stauber and Müller, 2008), which allows researchers to use the same sample for additional analyses. At last, micro-CT can acquire much higher resolution models than clinical CT scanners. A study showed when comparing the laying hen bone analysis results from clinical CT and micro CT, moderate to weak correlations on tibia bone area were observed, which may be due to the low resolution of clinical CT that caused partial volume effects (Regmi et al., 2017).

By applying the bone separation, the different parts of bones can be isolated and analyzed individually to get more sophisticated data, such as trabecular bone thickness (**Tb.Th**), trabecular bone separation (**Tb.Sp**), trabecular number, and so on (**Tb.N**) (Buie et al., 2007). Studies have shown the increase of total laying hen BMD is not highly associated with resistance to osteoporosis because an increase in overall BMD may be mainly contributed by the rise of medullary bone formation (Korver et al., 2004). The ability of micro-CT to distinguish different parts of bones will allow us to test this assumption. However, the separation of cortical, trabecular, and medullary bones of mature laying hens is difficult compared to mouse or rat bones because of the presence of medullary bones. Furthermore, owing to the long scanning time and high resolution, lots of

factors such as the temperature, sample movement, misalignment, beam hardening, dust on the sensory, and so on have significant impacts on outcomes (Ritman, 2004). At last, the micro-CT has a relatively small chamber for holding the samples, which limits the bone size for scanning. Nevertheless, the capacity of micro-CT to distinguish different bone fractions will provide more valuable aspects in laying hen bone health assessment and allow the researcher to observe the detailed changes in bone structures. This technique will significantly expand our understanding of chicken bone physiology and osteoporosis.

THE PROCEDURE OF MICRO-CT ON LAYING HEN BONE ANALYSIS

Sample preparation and installation for scanning

The adult laying hen bones are relatively larger than the mice or rat bones. The length of the modern layer femurs from 1-day-old to 95-week-old birds is shown in Figure 1. This figure shows the bone length reaches its peak at sexual maturity (around 18 wk of age). During the laying period, the bone length is consistent agreeing with the previous reviews (Whitehead and Fleming, 2000; Whitehead, 2004; Fleming et al., 2006). For a micro-CT scanner, a low-radio dense sample holder is used based on the length of bones and the chamber size. The larger layer bone results in longer scanning time compare to mice or rats; thus, the extra attention to avoiding dehydration of specimen during the scanning needs to be addressed. Several media can be used, including ethanol, saline, or water. However, different media affect x-ray attenuation (Nazarian et al., 2008). The scanning media must be constant throughout the samples. The soft tissues need to be carefully removed to avoid any effects on the x-ray attenuation of bones.

The samples should be firmly positioned in the holder with the same horizontal axis (Bouxsein et al., 2010).

Image acquisition for laying hen bones

The attenuation of the x-ray photons results from either absorption or scattering depending on the energy (Grodzins, 1983). The photon energy is expressed as units of electronvolts (eV). A rule for selecting energy of photons is that the thicker and denser samples require higher energy (Bouxsein et al., 2010). Mice have a smaller bone with a diameter less than 3 mm (Martín-Badosa et al., 2003), and a typical human long bone diameter is around 100 to 200 mm (Irie et al., 2018). However, the laying hen bone used for analysis usually has a higher diameter than that of the mice and rats, but less than that of humans. The width of laying hen femur from one-day-old to 95-week-old birds is shown in Figure 2. The photons' energy should be relatively higher than that of the mice or humans because of the longer travel distance of x-ray inside the laying hen bones (Grodzins, 1983). The photons' energy is further increased when the medullary bones were present in the cavity, as the medullary bone is highly mineralized (Dacke et al., 1993).

The intensity (number of photons during one projection) depends on current (μA), the exposure time (ms), and the frame averaging (number of pictures per rotation) (Bouxsein et al., 2010). The signal to noise ratio can be improved by increasing the exposure time and the average frame, but this will result in longer scanning time (Ritman, 2004). As the length of laying hen bones is usually longer than that of the mice and rats, the scanning time needs to be increased, which may result in a higher incident of misalignment and thermal drift during the scanning (Sasov et al., 2008). A mathematical post-alignment calibration needs to be applied for this scenario. An alternative way to reduce the scanning time is to shrink the scanning region and only focus on the region of interest (**ROI**) vs. the whole bone.
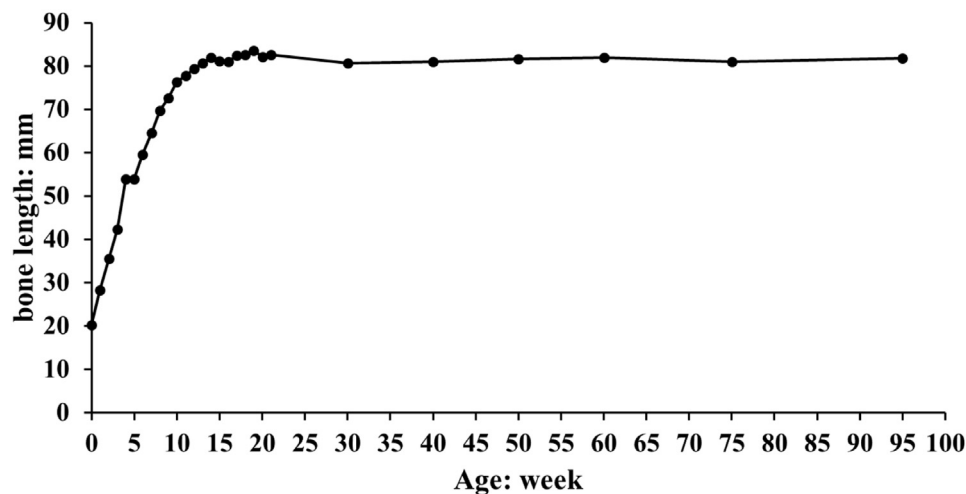

Figure 1. One-day-old Hy-line W36 layers were raised under the standard management and feeding program based on Hy-line W36 guide (2015) from 0 to 95 wk. During the experimental period, 10 birds' femur/time points were collected. The bone length was measured using a caliper (Mitutoyo 500-196-30, Aurora, IL).
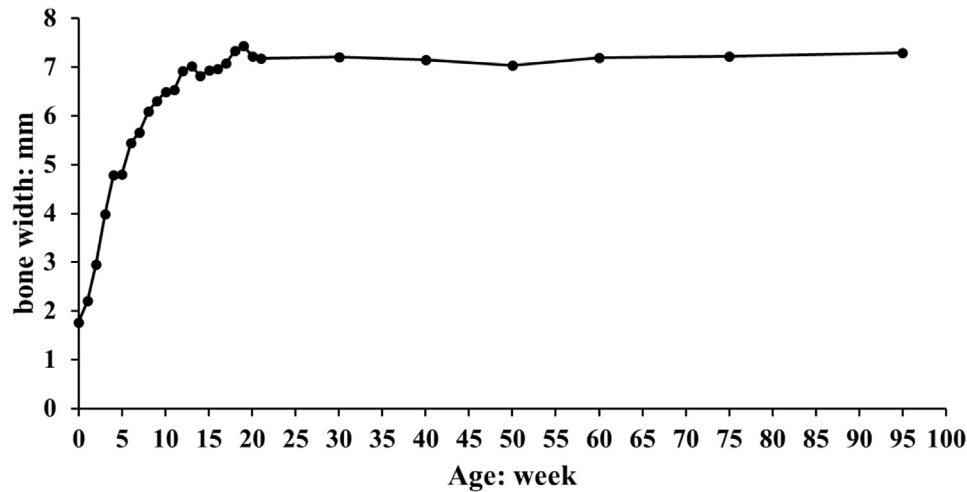
Figure 2. One-day-old Hy-line W36 layers were raised under the standard management and feeding program based on Hy-line W36 guide (2015) from 0 to 95 wk. During the experimental period, 10 birds' femur/time points were collected. The bone width was measured using a caliper. (Mitutoyo 500-196-30, Aurora, IL).

The voxel size can affect the accuracy of the analysis outcome. In general, the minimum ratio of voxels to the smallest structure size in an object is 2:1 (Bouxsein et al., 2010). The finest structure (trabecular bone) in mice bones is around 20 to 30 μm (Martín-Badosa et al., 2003). However, for laying hens, the trabecular thickness is between 60 and 220 μm. Therefore, the scanning resolution setting for laying hen bones can be lower than that of mice or rats. The subtle changes in high-resolution scanning will not significantly affect the results on relatively large structures (Müller et al., 1996). Therefore, the resolution setting in laying hen bone scanning may have higher forgiveness. However, both young pullets and aged laying hens have thin trabecular bones. Thus, the trabecular bone volume fraction to the total bone can be extremely low (Glatt et al., 2007). In this case, the scanning resolution needs to be increased accordingly. Besides, if the research interests are on the medullary bone structure, the pixel size needs to be reduced further as the medullary bone has a much smaller structure size (Kerschnitzki et al., 2014).

The volume of interest selection for laying hen bones

Based on research objectives, different parts of laying hen bones could be used. The humerus, tibia, femur, and keel bones are the most common bones used in laying hen research. Keel and humerus bones have become more and more popular in the free-range and aviary system studies because of the importance of these bones in cage-free systems (Whitehead and Fleming, 2000; Guesdon et al., 2004; Stratmann et al., 2015). However, to understand the basic metabolism of bones, the tibia and femurs with the presence of all 3 types of bone structures could be the research of interest (Whitehead, 2004). While considering the chamber size of micro-CT and a relatively large number of studies reporting the results from the femurs (Bouxsein et al., 2010), the femur

probably is one of the optimal choices for laying hen bone studies. However, because the shape of the femur is usually curved, the angle of the bone axis needs to be carefully adjusted before selecting a ROI.

The volume of interest (**VOI**) should represent the overall bone structures. The trabecular bone structures became less and less from the bone head to the diaphysis (Rosen et al., 2009). The extended VOIs may "dilute" the trabecular bone volume fraction to the total bone then mask the relevant difference between the treatments (Figure 3). However, the medullary bone has filled up the whole bone cavity evenly. A representative 60-week-old laying hen bone was scanned and analyzed to demonstrate the dilution of trabecular bone (Figure 3). As the medullary, trabecular, and cortical bones are equally crucial for layer bone research, the metaphysis would be a more represented region for hen bone studies. However, the height of VOI needs to be carefully decided to avoid the dilution of trabecular bones.

While considering the reproducible landmark for VOI, the nutrient foramina on the distal part of the femur head can be used, as it is shown continuously in this region (Figure 4A). However, in younger birds, the blood vessels do not occupy the bones, but in older birds, several nutrient foramina are shown in this region (Figure 5). In this case, another landmark can be used, which is described in Figure 4B. Both methods require the position of the bone to be at a certain angle in 3D space to make sure that the selection of VOIs is constant.

Laying hen bone model reconstruction

Acquired images need to be reconstructed to a 3D model before analysis. During the reconstruction, beam-hardening artifacts (the edges of an object to appear brighter than the center), ring artifacts (ring-like appearance on cross-section imaging), background noises (grainy appearance on cross-sectional imaging), and thermos drift (blurry image caused by the movement of X-ray source
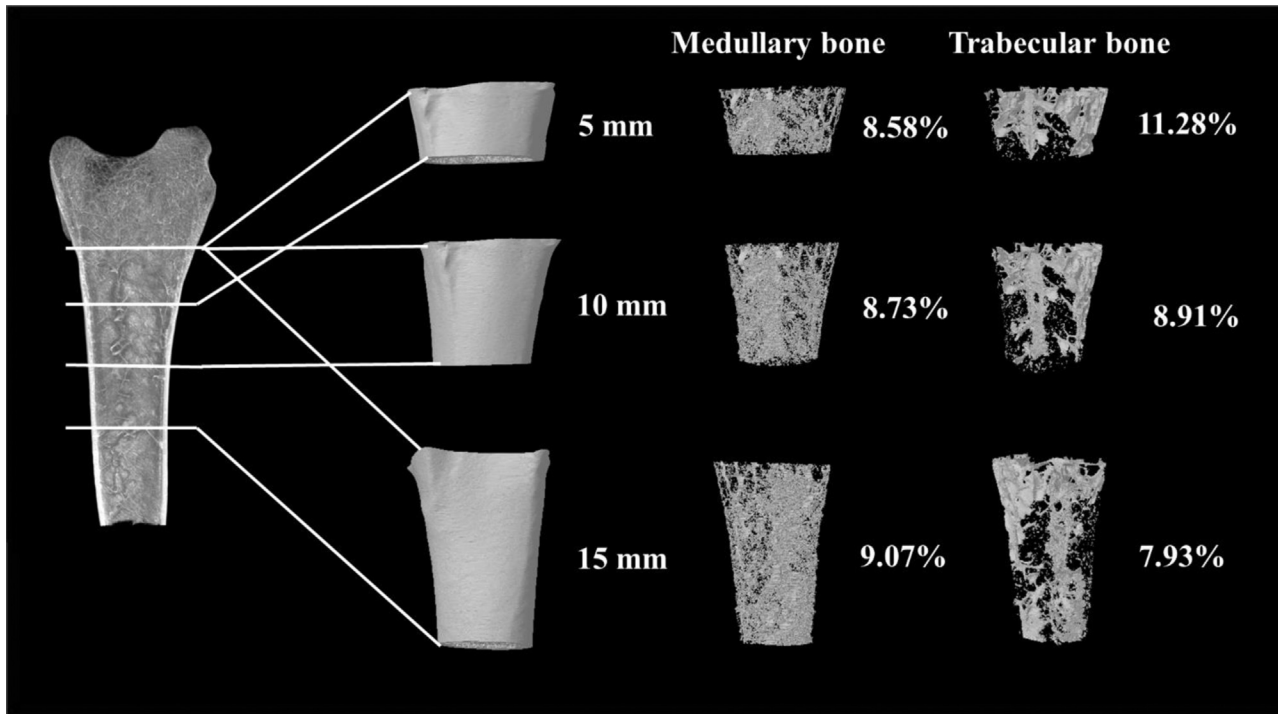
Figure 3. A representative 60-week-old Hy-line W36 laying hen's femur was used to demonstrate the dilution effects showed in laying hen bone (Laying hens are raised under the standard feeding and management program.). The bones were scanned by using a micro-computed tomography (micro-CT) scanner (Skyscan 1275; Bruker micro-CT, Belgium) and reconstructed using NRecon (version: 1.6.10.5; Bruker micro-CT, Belgium). The volume of interest (VOI) was selected starting from a nutrient foramen using data viewer (version: 1.5.2.4; Bruker micro-CT, Belgium; see the introduction in Figure 5); 5 mm, 10 mm, and 15 mm were selected as VOI followed by a segmentation analysis (CTan, version: 1.16.4.1; Bruker micro-CT, Belgium). The numbers showed the ratio of parts bone volume (medullary bone or trabecular bone) vs. total bone volume. The analysis showed there are almost no changes in medullary bone percentage when expending the VOI, but a trend of decrease of trabecular bone ratio was detected.
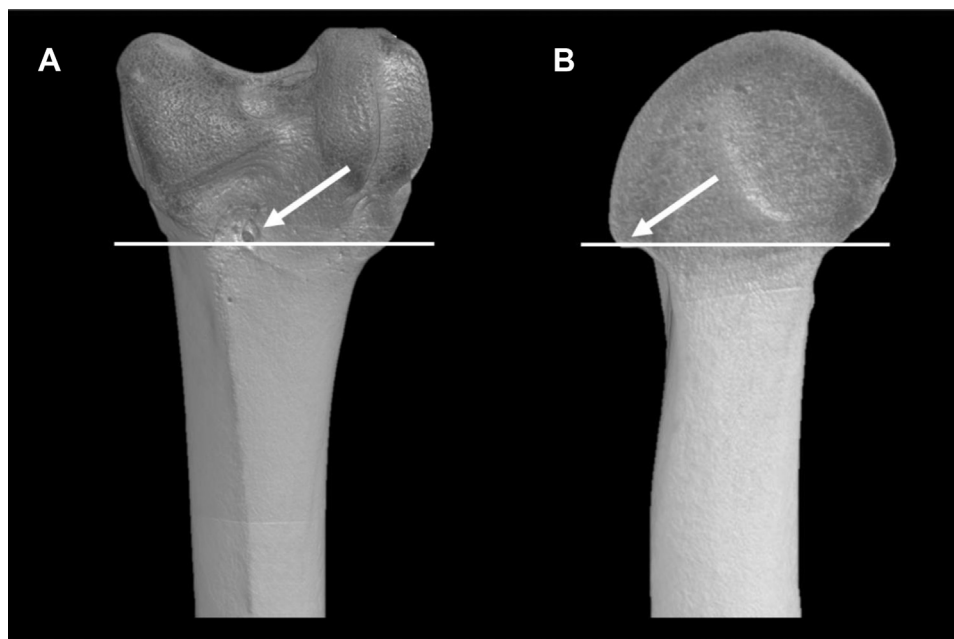

Figure 4. Two 60-week-old Hy-line W36 laying hens' femur femora distal metaphysis images (Skyscan 1275; Bruker micro-CT, Belgium) were showed to demonstrate the potential landmarks (arrows) that can be used in volume of interest (VOI) selection: (A) the nutrient foramen presented in the bonehead at a similar position regularly. A VOI selection can be made from there or a certain distance from there to avoid including any holes inside the VOI. (B) For young and old birds; the widest part of the bonehead showed in the pictures could be used as the landmark for the start of VOI selection.
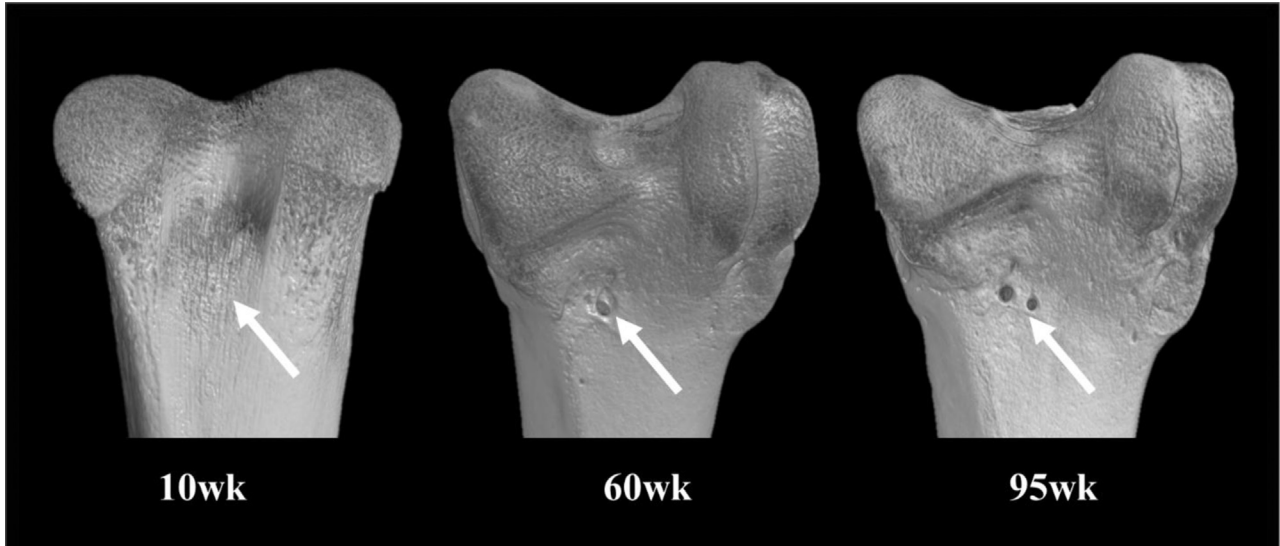
Figure 5. The femur from 10-week, 60-week, and 95-week-old Hy-line W36 layers (under standard management and feeding program) was scanned (Skyscan 1275; Bruker micro-CT, Belgium) and shown in the picture. The nutrient foramen (arrow) has not developed at the young age of birds, and multiple nutrient foramens usually showed at aged birds.

due to heat) need to be checked carefully (Bouxsein et al., 2010). The mathematical corrections are performed using software programs (Bouxsein et al., 2010). The metal artifacts are not typical for the laying hens. Instead, the motion artifact is the most frequent issue during the laying hen oversize scanning, which results from sample movement or camera thermos drift.

THE AUTOMATED BONE SEPARATION ALGORITHMS FOR LAYING HEN BONES

Bone separation could be achieved by manually drawing the ROI slice by slice or using automated algorithms (Buie et al., 2007; Kohler et al., 2007; Ang et al., 2020).

There are no available automated algorithms for laying hen bone separation in previous reports. Even manual separation is difficult when the trabecular bones and medullary bones are present at the same time. Our automated separation algorithms are designed based on the morphology difference of medullary bone compared to trabecular and cortical bones. The medullary bone has 2 primary forms in the bones (Figure 6). During the early laying period, it shows as delicate loosely woven bones distributed throughout the cavity, which could be separated by applying different thresholds. However, during the late laying period, most of the time, the medullary bone clustered together to form calcium chunks, which are hard to separate by applying different thresholds.
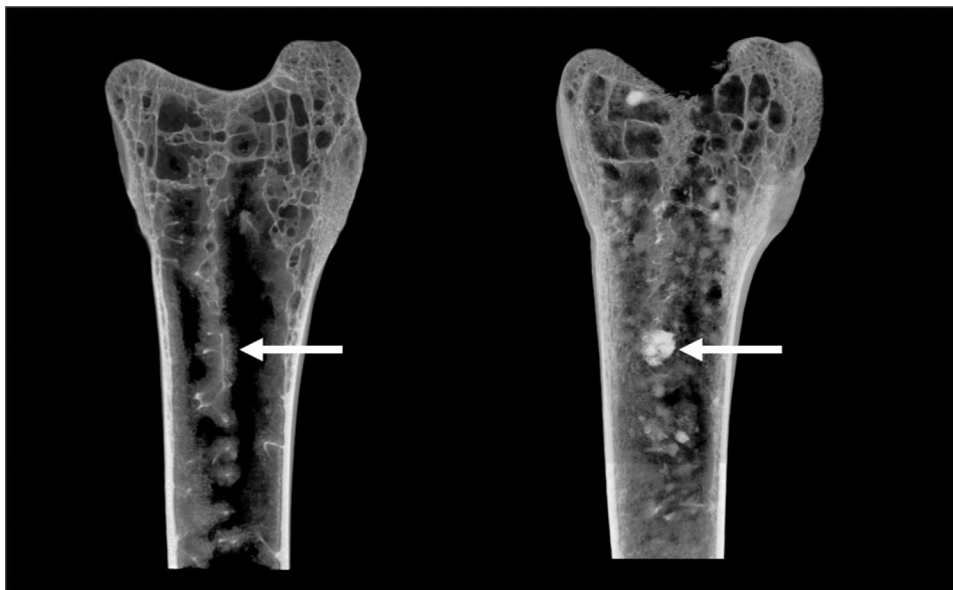

Figure 6. Two representative bones were scanned (Skyscan 1275; Bruker micro-CT, Belgium) and presented using CTvox (version: 3.2.0 r1294; Bruker micro-CT, Belgium) to show the type of structure of medullary bone (arrow). Left: 20-week-old Hy-line w36 laying hen femur with the delicate loosely woven bones distributed throughout the cavity; right: 95-week-old Hy-line w36 laying hen femur with the medullary bone clustered together to form calcium chunks.

In this case, we defined the diameter of medullary chunks as higher than the trabecular bone thickness as a separation trait. The opening or closing procedure was used for the separation. It needs to be noticed that, if a medullary bone chunk binds with the trabecular structure, this separation may result in artificial damages on trabecular bone structures, which will affect the connectivity of trabecular bones. This automated bone separation process has combined both situations along with some additional processes to avoid errors such as holes on the
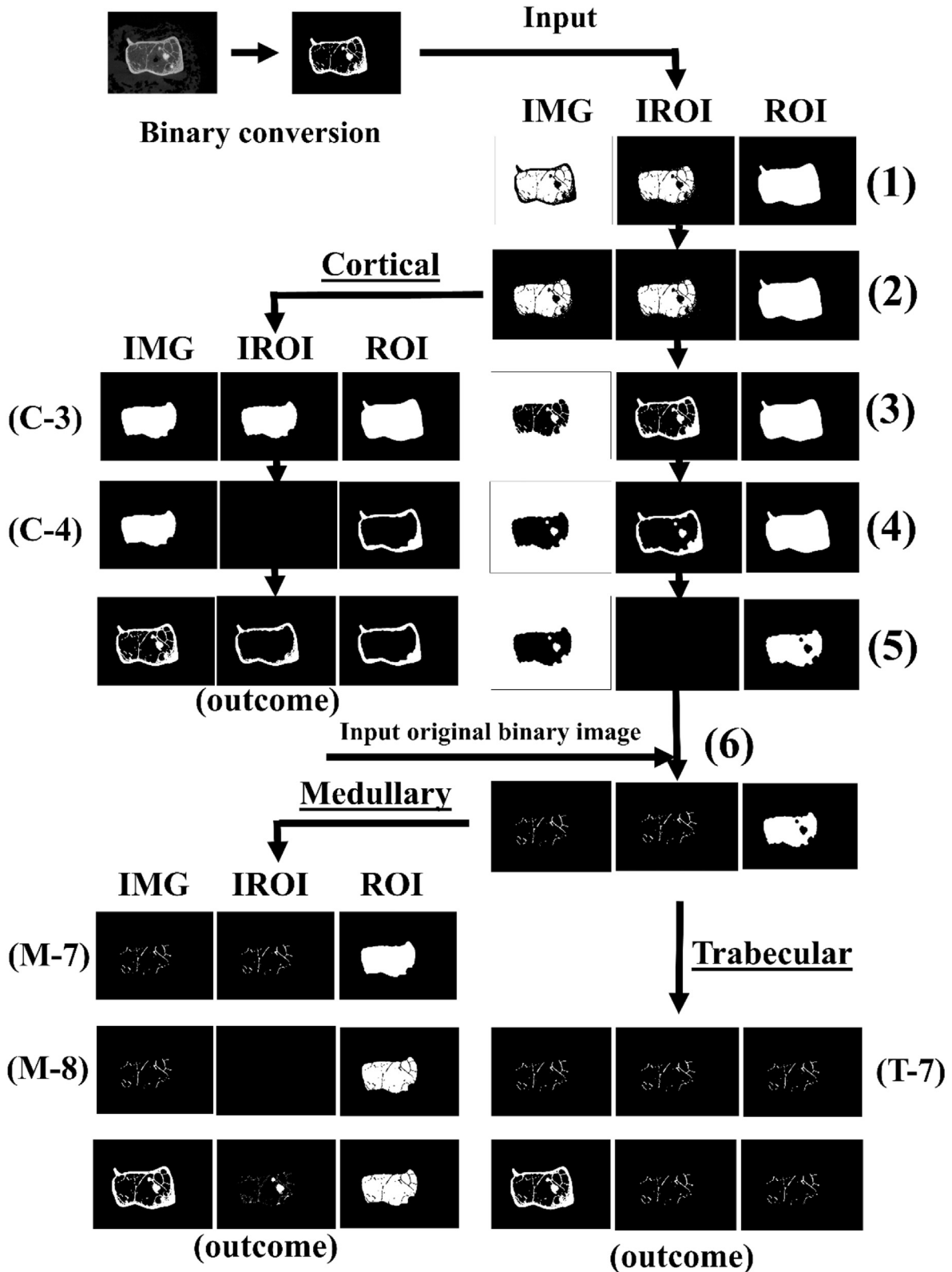

Figure 7. The diagram showed the critical step of the automatic bone separation procedure to better understand the process. Three types of views were presented in the diagram: IMG: view of the image; IROI: view of the image inside ROI (region of interest); ROI: view of ROI.

cortical bones, foreign matters around the object, and so on.

A diagram is presented to show the critical steps of the automated bone separation procedure (Figure 7). First, the image is converted to the binary picture by applying (global) threshold, followed by a despeckle to remove everything foreign except for the most massive object in 3D space for a cleaner scan. The following steps summarize the whole process:

Step (1). Region of interest (ROI) shrink-wrap: ROI is shrunk-wrapped in 2D space with stretching over the holes to avoid any leaking of ROI inside the bone cavity due to the holes in the bones. After this step, the air around the object is excluded.

Step (2). Bitwise operations: Image = NOT image followed by image = image AND ROI. A small opening followed by despeckling is recommended at this step to remove any pixels that potentially exist around the object because of the stretching over the hole's functions.

Step (C-3). A closing procedure on the image at 2D space with a large radius is applied. The minimum radius setting should be larger than the thickest trabecular bone. Erosion of ROI is recommended to let ROI a few pixels away from the endocortical surface to make sure all the cortical bones have been selected.

Step (C-4). Bitwise operation: ROI = ROI SUB image. The final ROI is defined. After reloading the image, the final cortical bone separation outcome is shown in the picture.

Step (3). Bitwise operation: Image = NOT image. This process makes trabecular bone in the image artificially connected to the air around to avoid being removed by the next procedure.

Step (4). An opening is provided on the image at 2D space with a radius set between the diameter of medullary calcium chunk and the thickness of the trabecular bone. Usually, the diameter of the chunk is much higher than trabecular bone thickness. This procedure is optimal to separate the calcium chunk and trabecular bone.

Step (5). Bitwise operation: ROI = ROI SUB Image. A small erosion of ROI is recommended after this step. The erosion procedure can shrink the ROI selection to make it a few pixels away from calcium chunk. This erosion avoids trabecular ROI, including a "calcium shell" pealed from calcium chunk, which is due to the calculation error of the opening procedure.

Step (6). The original binary image is reloaded in the process of further assisting ROI determination. Afterward, a bitwise operation is applied: Image = Image AND ROI.

Step (M-7). A closing procedure was performed on ROI to fill the unselected calcium chunk region.

Step (M-8). Bitwise operation: ROI = ROI SUB image is applied to finalize the ROI for medullary bone selection.

Step (T-7) ROI = image. The ROI of the trabecular bone region is determined.

This automated algorithm separates the major bones of each part (Figure 8), and the progress is logical and reasonable. There is no human bias while applying it to all the samples. The bones from laying hens at age 17, 20, 30, 40, 60, 75, and 95 wk (10 bones/week) have been fitted in this algorithm. Grubbs' test was applied to examine the outcome for cortical, trabecular, and medullary bone volume and BMD at each age (n = 10). The significant level was set at a P value of less than 0.05 to detect outliers. Results showed that no outlier was detected, indicating that the separation was stable and accurate. A similar method has been applied in another laying hen study. Castro et al. (2019) reported that the laying hen fed 100% required total sulfur amino acid (**TSAA**) had higher egg production than the one fed 70% TSAA. Higher egg production may reduce stored Ca in the medullary bone because of resorption driven by eggshell formation. In the same experiment, lower medullary BMD was found in the same treatment (100% TSAA) using micro-CT (Castro et al., 2019). Future work will focus on comparable research methods to further validate the current methods and confirm the current algorithm.

CONCLUSION

The size of hen bone and the exhibition of medullary bone inside the bone marrow cavity are major factors distinguishing the application of micro-CT on birds from other mammals. Compared to other small animals such
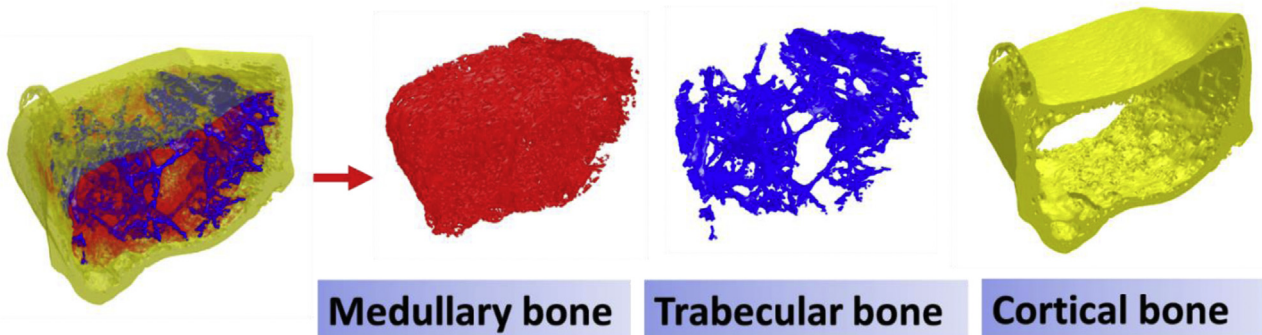

Figure 8. The diagram shows an example of laying hen bone separation outcome. The bone was processed according to the methods indicated in the article. The pictures were made using CTvol (version: 2.3.2.0; Bruker micro-CT, Belgium).

as mouse and rat, while applying micro-CT in laying hen bone research, many settings and potential issues were indicated in the current review. In general, a scanning setting for laying hen bone should consider the contrast of the image, the possible artifacts, and the balance of the scanning time and file size. An automated laying hen bone separation process is presented for the very first time. It provides the possibility and progress on advancing laying hen bone analysis. The algorithm for bone separation should consider the complexity of medullary bone structures. Dual threshold needs to be used to separate the woven bones such as medullary bones. Meanwhile, closing and opening procedures should be used to separate the medullary calcium clusters that are binding on trabecular bone. A recent study demonstrated that laying hen bones at various ages were fitted in the program. No outlier was observed in this trial, indicating that the separation process is stable and accurate. Micro-CT, as a powerful bone-assessment tool, will contribute to poultry bone studies and provide critical insight for enhancing our understanding of skeletal integrity and improving welfare of poultry.

ACKNOWLEGMENTS

REFERENCES

Ang, I., C. M. Fox, J. D. Polk, and M. E. Kersh. 2000. An algorithm for automated separation of trabecular bone from variably thick cortices in high-resolution computed tomography data. IEEE Trans. Biomed. Eng. 67:924–930.

Bouxsein, M. L., S. K. Boyd, B. A. Christiansen, R. E. Guldberg, K. J. Jepsen, and R. Muller. 2010. Guidelines for assessment of bone microstructure in rodents using micro-computed tomography. J. Bone Miner. Res. 25:1468–1486.

Buie, H. R., G. M. Campbell, R. J. Klinck, J. A. MacNeil, and S. K. Boyd. 2007. Automatic segmentation of cortical and trabecular compartments based on a dual threshold technique for in vivo micro-CT bone analysis. Bone 41:505–515.

Castro, F. L. S., H. Y. Kim, Y. G. Hong, and W. K. Kim. 2019. The effect of total sulfur amino acid levels on growth performance, egg quality, and bone metabolism in laying hens subjected to high environmental temperature. Poult. Sci. 98:4982–4993.

Dacke, C., S. Arkle, D. Cook, I. Wormstone, S. Jones, M. Zaidi, and Z. Bascal. 1993. Medullary bone and avian calcium regulation. J. Exp. Biol. 184:63–88.

Feldkamp, L. A., S. A. Goldstein, M. A. Parfitt, G. Jesion, and M. Kleerekoper. 1989. The direct examination of three-dimensional bone architecture in vitro by computed tomography. J. Bone Miner. Res. 4:3–11.

Fleming, R. H., H. A. McCormack, L. McTeir, and C. C. Whitehead. 2006. Relationships between genetic, environmental and nutritional factors influencing osteoporosis in laying hens. Br. Poult. Sci. 47:742–755.

Glatt, V., E. Canalis, L. Stadmeyer, and M. L. Bouxsein. 2007. Age-related changes in trabecular architecture differ in female and male C57BL/6J mice. J. Bone Miner. Res. 22:1197–1207.

Grodzins, L. 1983. Optimum energies for x-ray transmission tomography of small samples: applications of synchrotron radiation to computerized tomography I. Nucl. Instrum. Methods Phys. Res. 206:541–545.

Guesdon, V., C. Leterrier, P. Constantin, D. Guémené, M. Couty, and J. M. Faure. 2004. Humeral quality and adrenal responsiveness in laying hens reared in standard and furnished cages. Anim. Res. 53:235–243.

Irie, M. S., G. D. Rabelo, R. Spin-Neto, P. Dechichi, J. S. Borges, and P. B. F. Soares. 2018. Use of micro-computed tomography for bone evaluation in Dentistry. Braz. Dent. J. 29:227–238.

Kerschnitzki, M., T. Zander, P. Zaslansky, P. Fratzl, R. Shahar, and W. Wagermaier. 2014. Rapid alterations of avian medullary bone material during the daily egg-laying cycle. Bone 69:109–117.

Kim, W. K., S. A. Bloomfield, T. Sugiyama, and S. C. Ricke. 2012. Concepts and methods for understanding bone metabolism in laying hens. Worlds. Poult. Sci. J. 68:71–82.

Kohler, T., M. Stauber, L. R. Donahue, and R. Muller. 2007. Automated compartmental analysis for high-throughput skeletal phenotyping in femora of genetic mouse models. Bone 41:659–667.

Korver, D. R., J. L. Saunders-Blades, and K. L. Nadeau. 2004. Assessing bone mineral density in vivo: quantitative computed tomography. Poult. Sci. 83:222–229.

Martín-Badosa, E., D. Amblard, S. Nuzzo, A. Elmoutaouakkil, L. Vico, and F. Peyrin. 2003. Excised bone structures in mice: imaging at three-dimensional synchrotron radiation micro CT. Radiology 229:921–928.

Müller, R., B. Koller, T. Hildebrand, A. Laib, S. Gianolini, and P. Rüegsegger. 1996. Resolution dependency of microstructural properties of cancellous bone based on three-dimensional μ-tomography. Technol. Health Care 4:113–119.

Nazarian, A., B. D. Snyder, D. Zurakowski, and R. Müller. 2008. Quantitative micro-computed tomography: a non-invasive method to assess equivalent bone mineral density. Bone 43:302–311.

Reich, T., and A. Gefen. 2006. Effect of trabecular bone loss on cortical strain rate during impact in an in vitro model of avian femur. Biomed. Eng. Online 5:45.

Regmi, P., A. G. Cox, C. I. Robison, and D. M. Karcher. 2017. Correlation analysis of cortical geometry of tibia and humerus of white leghorns using clinical quantitative computed tomography and microcomputed tomography scans. Poult. Sci. 96:2950–2955.

Ritman, E. L. 2004. Micro-computed tomography—current status and developments. Annu. Rev. Biomed. Eng. 6:185–208.

Ritman, E. L. 2007. Small-animal CT: its difference from, and impact on, clinical CT. Nucl. Instrum. Meth. A. 580:968–970.

Rosen, C. J., J. E. Compston, and J. B. Lian. 2009. ASBMR Primer on the Metabolic Bone Diseases and Disorders of Mineral Metabolism. John Wiley & Sons, Hoboken, NJ.

Schambach, S. J., S. Bag, L. Schilling, C. Groden, and M. A. Brockmann. 2010. Application of micro-CT in small animal imaging. Methods 50:2–13.

Siffert, R., G. Luo, S. Cowin, and J. Kaufman. 1996. Dynamic relationships of trabecular bone density, architecture, and strength in a computational model of osteopenia. Bone 18:197–206.

Stauber, M., and R. Müller. 2008. Micro-computed tomography: a method for the non-Destructive evaluation of the three-dimensional structure of Biological specimens. Pages 273–292 in Osteoporosis: Methods and Protocols. J. J. Westendorf, ed. Humana Press, Totowa, NJ.

Sasov, A., X. Liu, and P. L. Salmon. 2008. Compensation of mechanical inaccuracies in micro-CT and nano-CT. In Proc. SPIE 7078, Developments in X-Ray Tomography VI, 70781C. S. R. Stock, ed. The International Society for Optics and Photonics, Bellingham, Washington.

Stratmann, A., E. K. F. Fröhlich, S. G. Gebhardt-Henrich, A. Harlander-Matauschek, H. Würbel, and M. J. Toscano. 2015. Modification of aviary design reduces incidence of falls, collisions and keel bone damage in laying hens. Appl. Anim. Behav. Sci. 165:112–123.

Webber, C. E., C. L. Gordon, and P. S. Nicholson. 1998. Relation between image-based assessment of distal radius trabecular structure and compressive strength. Can. Assoc. Radiol. J. 49:390.

Whitehead, C. 2004. Overview of bone biology in the egg-laying hen. Poult. Sci. 83:193–199.

Whitehead, C., and R. Fleming. 2000. Osteoporosis in cage layers. Poult. Sci. 79:1033–1041.